

STEM VASCULAR ARCHITECTURE IN THE RATTAN PALM *CALAMUS* (ARECACEAE–CALAMOIDEAE–CALAMINAE)¹

P. BARRY TOMLINSON,^{2,5} JACK B. FISHER,³ RUSSELL E. SPANGLER,⁴ AND
RENEE A. RICHER⁴

²Harvard Forest, Harvard University, Petersham, Massachusetts 01366 USA; ³Fairchild Tropical Garden, 11935 Old Cutler Road, Miami, Florida 33156 USA and Department of Biological Sciences, Florida International University, Miami, Florida 33199 USA;

⁴Department of Organismic and Evolutionary Biology, Harvard University, Cambridge, Massachusetts 02138 USA

Climbing stems in the rattan genus *Calamus* can reach lengths of well over 100 m, are long-lived, and yet their vascular tissue is entirely primary. Such a combination suggests that stem vasculature is efficient and resistant to hydraulic disruption. By means of an optical shuttle and video recording of sequential images we analyzed the stem of a cultivated species. The stem has vascular features that are unusual compared with those in arborescent palms and seemingly inefficient in terms of long-distance water transport. Axial bundles are discontinuous basally because leaf traces, when followed downwards, always end blindly below. Furthermore, there is no regular distal branching of each leaf trace at its level of departure into a leaf, so that neither a continuing axial bundle nor bridges to adjacent axial bundles are produced as in the standard palm construction. Instead, the axial bundles in the stem periphery are connected to leaf traces and to each other by narrow and irregular transverse or oblique commissures that are not the developmental homologues of bridges. As in other palms, metaxylem within a leaf trace is not continuous into the leaf so that the only connection to a leaf is via protoxylem. Within the stem, protoxylem (tracheids) and metaxylem (vessels) are never contiguous, unlike in other palms, which suggests that water can only move from metaxylem to protoxylem, and hence into the leaf, across a hydraulic resistance. We suggest that this minimizes cavitation of vessels and/or may be associated with an unknown mechanism that refills embolized vessels. Also, the metaxylem can be significant in stem water storage in the absence of abundant ground parenchyma.

Key words: Arecaceae; *Calamus*; hydraulic architecture; liane; palm; rattan; vascular system; vessels.

“Rattan” is the colloquial name given to a large group of climbing palms whose stems have wide use as commercial canes (rattan in a manufacturing sense). In this paper we demonstrate that their stem vascular system differs substantially from other palms in ways that suggest a discontinuous method of long-distance water transport. The discontinuity results from the absence of conspicuous interconnections (bridges) between stem vascular bundles such as occurs in other palms, i.e., “tree palms” (Zimmermann and Tomlinson, 1965; Tomlinson, 1990, 1995). The absence of direct continuity is a surprising observation, since one would expect these high-climbing stems to have high conductive efficiency especially as they can, in some species, reach lengths of well over 100 m. Burkill (1966) records a cane whose length was measured at 556 feet, i.e., 170 m, with an even longer specimen destroyed by elephants before it could be measured. As we discuss later, the stems may be built with a higher than normal safety factor, since their vascular system is entirely primary and cannot be replaced or repaired.

The genus *Calamus* is the most species rich of all palms, by a considerable number, with an estimated 370 species, ~15% of all palms (Uhl and Dransfield, 1987). Their habit thus may be ecologically very successful even though some species are not high-climbing. *Calamus* is also one of seven climbing genera that constitute the subtribe Calaminae of the subfamily Calamoideae (Uhl and Dransfield, 1987). Molecular and morphological evidence indicates that the subtribe is monophyletic, but still only

one of several groups within the palms in which the scandent habit has evolved (Baker et al., 1999; Tomlinson and Fisher, 2000). The ecological success of the climbing habit in rattans, together with their commercial importance, suggests that a knowledge of stem vasculature could be important both practically and theoretically. Our present objective is to describe vascular interconnections of the mature climbing stems based on the analysis of a representative species and comparison with the stem of several others. Our research has been greatly facilitated by the detailed descriptions of rattan anatomy by Gudrun Weiner, which allow us to generalize from our detailed knowledge of one species to the genus as a whole (Weiner, 1992; Weiner and Liese, 1992, 1993). From her detailed survey of 284 species in 13 genera we understand that genera can be identified to a large extent from stem anatomy. We also have access to knowledge of the common anatomical features of rattan stems, and we have been provided with measurements of the quantitative variation in stem dimensions along a single cane. We thus are confident that our own detailed analysis of stem vasculature in one taxon has wider applicability in the genus as a whole, especially as many of the features that we now understand from our three-dimensional analysis can be recognized in single transverse and longitudinal sections. Furthermore, we can be confident that the vascular anomalies we describe here distinguish the rattans from other palms because our general understanding of palm stem vasculature (the “*Rhapis* model”) is quite comprehensive (Zimmerman, McCue, and Sperry, 1982; Zimmermann and Tomlinson, 1965; Tomlinson, 1990, 1995). The objective of our investigation has been, therefore, to add a three-dimensional and functional perspective to the observations of previous workers.

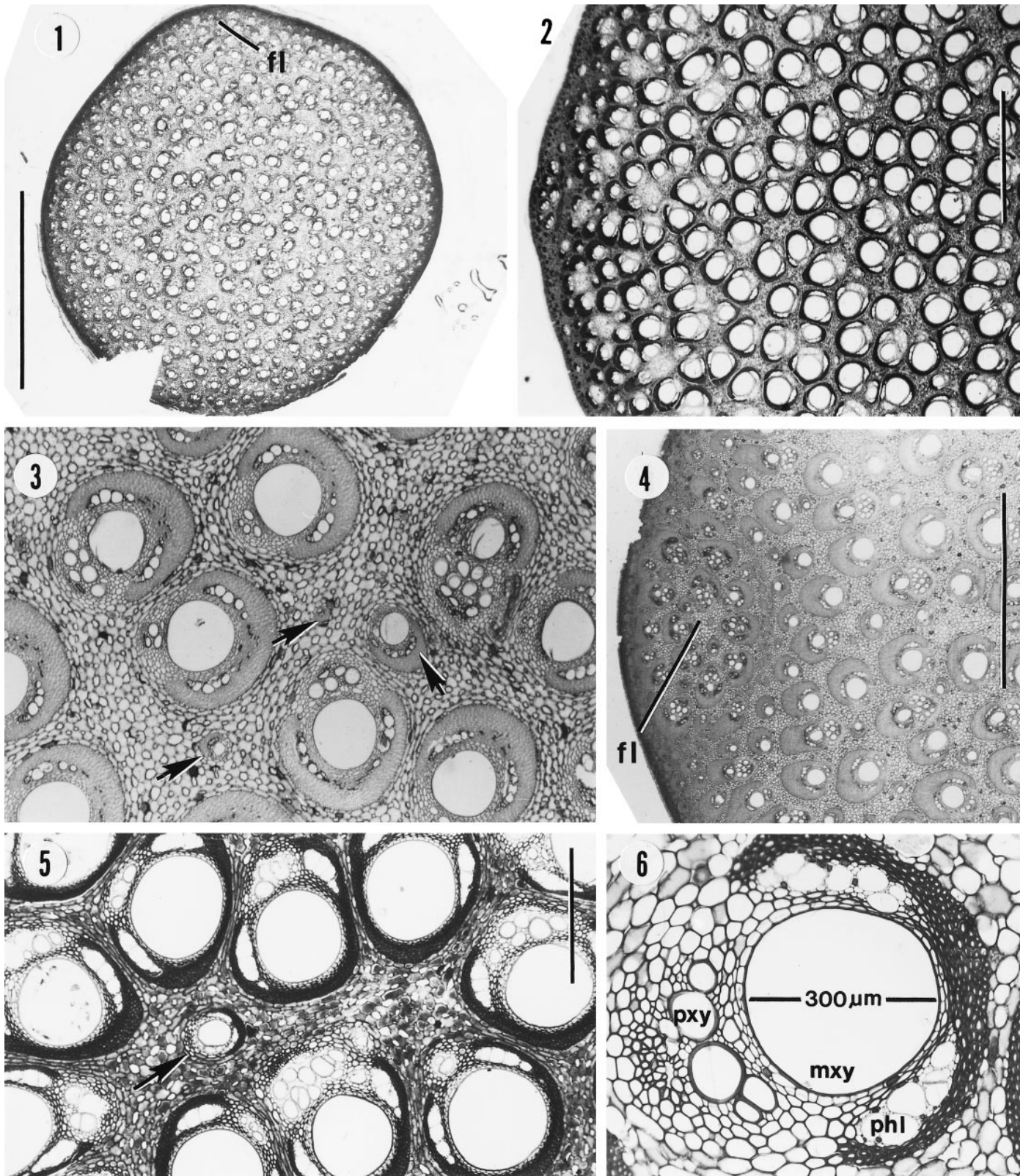
MATERIALS AND METHODS

Canes studied in detail were derived from a single rhizomatous clump cultivated at Fairchild Tropical Garden and identified as *Calamus longipinna* K.

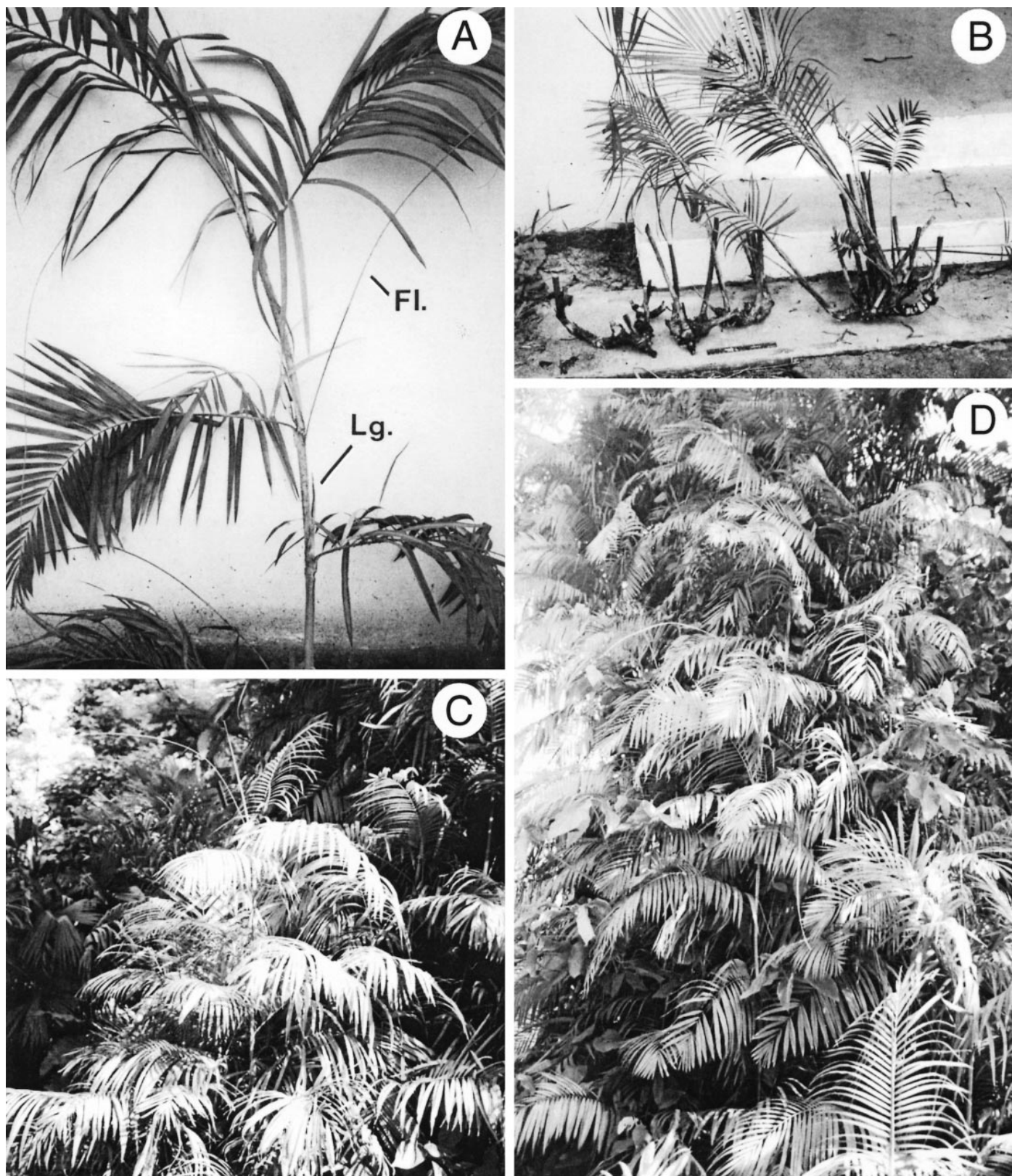
¹ Manuscript received 21 March 2000; revision accepted 18 July 2000.

The Harvard authors thank the Director, National Tropical Botanical Garden for accommodation in Miami at “The Kampong,” 4013 Douglas Road, Coconut Grove, Miami, Florida 33133 USA, and the Director, Fairchild Tropical Garden, for access to living specimens in its collections. We thank Gordon Lemon for use of the habit illustrations originating from a Harvard Summer School class project at Fairchild Tropical Garden.

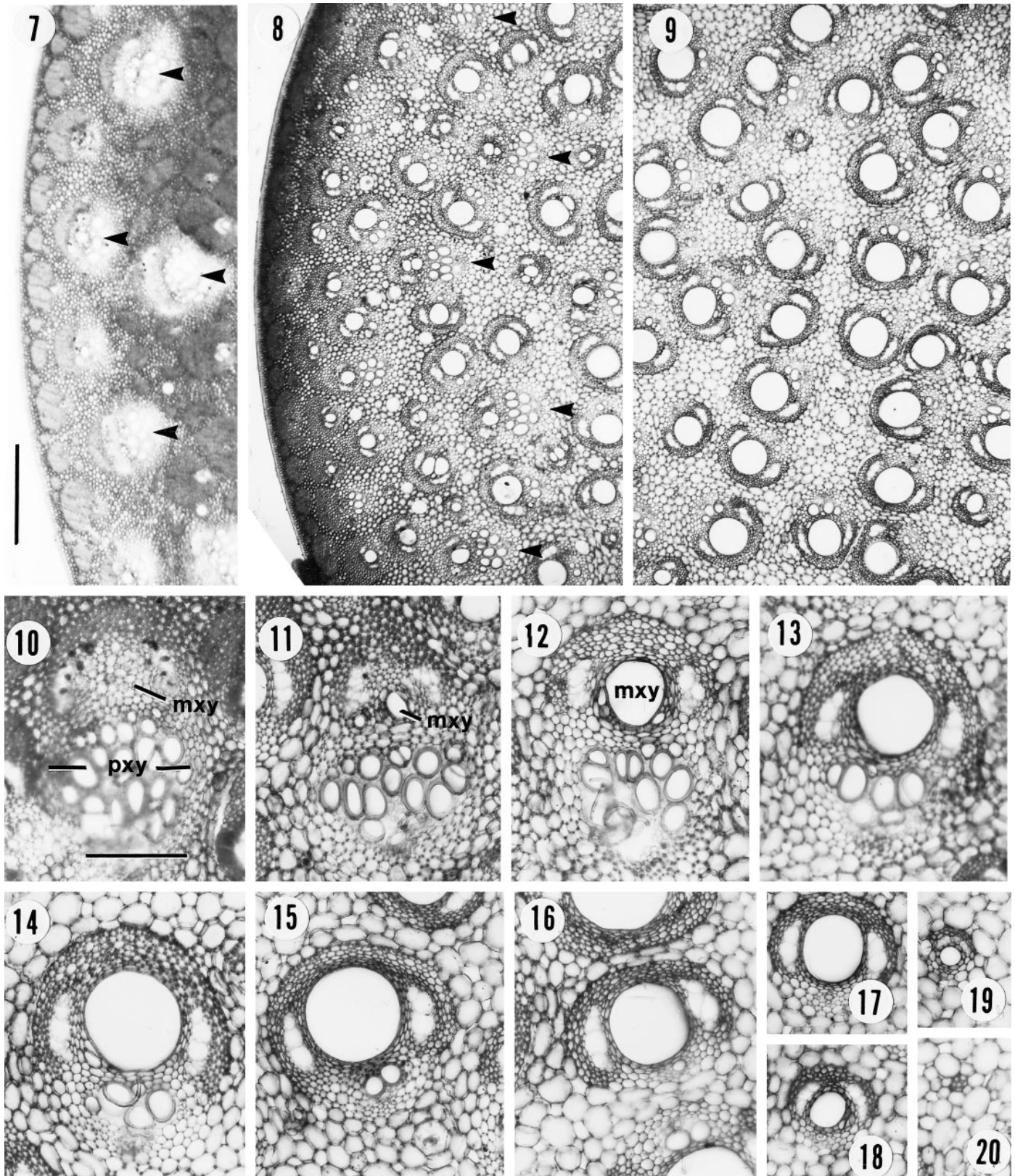
⁵ Author for correspondence (email: pbtomlin@fas.harvard.edu).



Figs. 1–6. *Calamus*. General features of stem anatomy. All transverse section. **1.** *Calamus longipinna* whole stem, flagellum (fl.) is prominent above, the notch cut for orientation below. Scale bar = 5 mm. **2.** *Calamus* sp. HEM 9264. Sector of stem to show relative uniform and dense vascular bundles; area metaxylem vessels to total stem area $\approx 30\%$ in stem center. Scale bar = 2 mm. **3.** *Calamus sciponium* stem center with ground tissue organization most characteristic of the genus. Arrows indicate small vascular bundles of various diameters that are also distinctive. **4.** *Calamus sciponium* stem periphery including adnate flagellum (fl.). Scale bar = 2 mm. **5.** *Calamus* sp. HEM 9264, stem center with congested vascular bundles, very wide metaxylem vessels $\approx 350 \mu\text{m}$ in diameter. Arrow shows distinctive narrow axial bundle. Scale bar = 500 μm . **6.** *Calamus deeratus*, single vascular bundle from stem center, with wide (300 μm) metaxylem (mxy) vessel. Phloem (phl) in two separated strands; protoxylem (pxy) not in contact with metaxylem. Scale bar in Fig. 6 is the same as for Fig. 3.



Figs. A–D. *Calamus longipinna*. Habit. **A.** Isolated shoot to show free portion of flagellum (Fl.) and ligule (Lg.). **B.** Disinterring rhizome system with young erect shoots. **C.** Clump of shoots in juvenile stage, the tallest shoot with its first flagellum. **D.** Older clump with many high-climbing shoots, the tallest reaching a height of ~12 m.



Figs. 7–20. *Calamus longipinna*. Bundle diversity. All transverse section. 7. Stem periphery with major leaf traces (arrowheads) obliquely entering stem; outer fibrous bundles corresponding to those of leaf sheath, cortex very narrow. Scale bar = 500 μ m. 8. Stem periphery towards middle of internode, major leaf traces that entered at node above marked by arrowheads. 9. Stem center, central bundles have no indication of overlapping vessel ends. Figs. 10–20. Series of photographs showing single bundle anatomy of progressively lower levels, all at same magnification. Scale bar = 200 μ m. The images do not show a single bundle but are representative of changes observed in one bundle traced continuously (cf. Fig. 43). Leaf trace in stem periphery just below node insertion

Schum & Lauterb. (J. Dransfield, Royal Botanic Gardens, Kew, personal communication) and grown from seed collected in Papua New Guinea. The specimen consists of numerous high-climbing canes, some of them tall enough to flower, growing into a large decaying live oak (Figs. A–D). Shoots of several sizes up to 10 m long and a relatively uniform diameter of 1–1.2 cm were sampled (Fig. 1). Additional material of other *Calamus* species was available in the palm slide collection of P.B.T., originating in Australia, Fiji, Malaysia, and West Africa, and demonstrated the constancy of vascular features at the generic level, but with a considerable range of dimensions. We have used some of this supplementary material to illustrate distinctive features of the genus as a whole (Figs. 2–6). This includes *Calamus* sp. HEM 9264, from Indonesia (Figs. 2, 5), *Calamus* cf. *sciponium* Lour., from an umbrella handle, from Malaysia (Figs. 3, 5) and *Calamus deeratus* Mann & Wendl., from West Africa (Fig. 6).

Fixation—For vascular analyses, mature canes up to 3.5 m long were cut into segment lengths of ~25 cm, the radial orientation of successive pieces being carefully recorded. Segments were tied together in bundles and fixed in FAA (85 parts 70% ethyl alcohol: 10 parts glacial acetic acid: 5 parts 40% formaldehyde). After fixation for several days material was transferred to 70% ethyl alcohol and subsequently in the laboratory washed well in running tap water prior to sectioning. Lengths of stem were chosen that had reached vegetative maturity, i.e., had adult leaf morphology and possessed well-developed flagella (sterile inflorescences), but were not flowering. Restriction avoided possible vascular complexities of juvenile stages or of stems at reproductive maturity. In addition, lengths of stem within the leafy crown were dissected to produce stem portions that included the shoot apex, leaf bases cut off shortly above the shoot apex, and several (up to ten) extending internodes. This material was embedded in paraffin wax and sectioned on a rotary microtome in the usual way. Results from the analysis of the developing regions were thus available to help understand the configuration of mature tissues but will be reported in detail in a later paper.

Sectioning—For mature stems, the texture of fully extended stem lengths starting two to three nodes below the first fully extended internode was most suited to free-hand sectioning. Here the vascular pattern is fully differentiated, but maturation of bundle sheath fibers and ground tissue is incomplete, since lignification of these tissues continues over many internodes (Bhat, Liese, and Schmitt, 1990). For vascular analysis over long distances sequential sections were cut at varying intervals, i.e., 0.1, 0.5, 1.0, 2.0 cm, with a short sequence of continuous sections cut at a thickness of 100 μm just below a node. The most useful section sequences for studying the overall course of vascular bundles were those cut at 1-cm intervals, in which continuity from section to section was easily retained. The shorter sequences gave detailed information about changes that occurred over short distances. The longest series cut (250 sections at 1-cm and 0.5-cm intervals) was from a cane 1.7 m long that included eight nodes (Figs. 39, 42). Individual bundles could be followed without interruption throughout this series.

Material was sectioned without embedding on a Reichert OME sliding microtome using a modified specimen holder that could clamp the longest segments. This also permitted the final cut to be made since a 1-cm length could still be clamped firmly. Sections were cut at thicknesses between 60 and 100 μm , since the primary purpose was to produce a complete section. Some tearing of the outer layers of the stem occurred, but this was not detrimental to the analysis, while thinner sections tended to fragment. Figures 7–20 are all taken from the sequence of sections used in the long-distance analysis.

Sections were stained for 1 min in 0.1% aqueous toluidine blue, rinsed in water, and mounted in dilute glycerine (glycerine : H₂O, 1 : 1) on frosted-ended slides labeled in pencil. Sections are semipermanent with little fading of the stain. Primary orientation of each section on the slide was provided by the prominent flagellum and a groove cut continuously from one stem segment to the next, the groove seen as a notch in each section (Fig. 1). Some of the shorter sequences were made permanent by tying them with cotton thread to the slide and double-staining them in a mixture of 1% safranin in 50% ethyl alcohol and aqueous alcian green (95 : 5 parts by volume), with routine methods of dehydration prior to mounting in Permout. Glycerine mounted preparations were most informative of histological features in a hydrated state as in most of our illustrations.

Maceration and clearing—Details of tracheary elements were studied in material macerated by boiling slivers in 10% potassium hydroxide for 3 min, rinsing well in water, and transferring to 20% chromic acid (aqueous chromium trioxide) for ~15 min. Softened material subsequently rinsed well in water was teased apart on slides in dilute glycerine for microscopic examination (Figs. 34–36). To study transverse commissures (vascular bundles interconnecting axial strands) thick longitudinal slices (i.e., 500 μm thick) of canes were cleared in a mixture of equal parts of aqueous 10% sodium hydroxide and 95% ethyl alcohol for several days, rinsed well in a water and 70% ethyl alcohol solution, and the clearing completed in lactic acid. After preliminary observations slices were stained in the same aqueous safranin/alcian green double stain and made permanent. The green stain emphasized the sieve-tubes of the phloem (Figs. 26, 28).

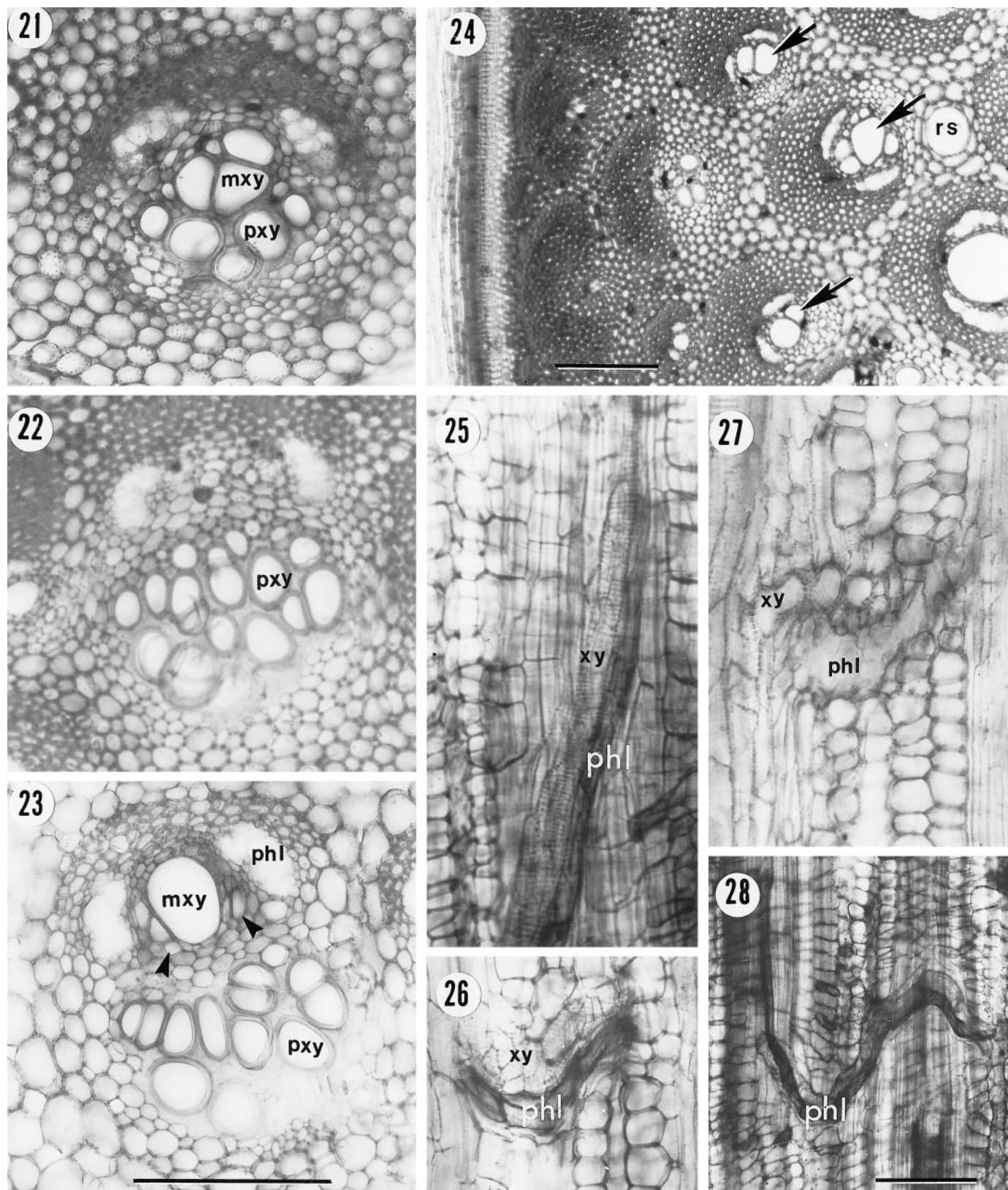
Vascular analysis—For quantitative analyses of the course of vascular bundles throughout the longest series, a modification of the cinematographic methods of Zimmermann and Tomlinson (1966) was used in which a video system was substituted for the optical camera in storing images. The optical shuttle microscope arrangement permitted precise alignment of images of successive sections; the video system permitted frame-by-frame (5 sec) recording of images, producing a tape that could be reviewed at any time and at variable speed, forwards and backwards so that continuity was directly observed. This supplied information used in the quantitative plots of Figs. 39–42, in which the emphasis is on histological changes within a vascular bundle throughout its length. Since the central bundles are longer than the longest stem analyzed, extrapolation from the upper end of one bundle to the middle and lower ends of other bundles was possible because the number of protoxylem tracheary elements in a bundle is a measure of its distance from insertion at a node, as explained later (Fig. 42). By adding from the same series the top of one bundle to the bottom of another, a reasonable measure of total vascular bundle length can be obtained (Fig. 43).

RESULTS

Morphology—The erect climbing stems of *Calamus* (Fig. A) arise from a somewhat irregularly branched sympodial rhizome system (Fig. B), which proliferates because each erect shoot is usually replaced by two or more, initially rhizomatous, renewal shoots. The rhizome system corresponds in principle to that system described for the small palm *Rhapis excelsa* (Tomlinson and Zimmermann, 1966), except that intervals between successive erect segments are much shorter (Fig. B). Rhizome anatomy is not considered here.

←

10. (cf. Fig. 7). Protoxylem (pxy) well developed; metaxylem absent, its position represented by parenchyma (mxy). 11. Leaf trace nearer stem center, metaxylem present as several narrow tracheary elements. 12. Leaf trace toward base of internode below node of insertion, metaxylem vessel single and wide but with adjacent transition tracheids. Protoxylem diminished. 13. Leaf trace (axial bundle) in stem center, at node below level of insertion; metaxylem vessel approaching maximum diameter, protoxylem further diminished. 14. Typical central bundle, maintaining this construction over several internodes. 15. Central bundle with reduced protoxylem. 16. Central bundle toward its base with reduced diameter and protoxylem of one narrow tracheid. 17. Narrower central bundle, metaxylem vessel narrowed; protoxylem almost absent. 18. Narrower central bundle without protoxylem. 19. Very narrow central bundle, basal extremity of an axial bundle. 20. Blind-ending axial bundle represented by fibers or parenchyma.



Figs. 21–28. *Calamus longipinna*. Details of vascular bundles in transverse section (Figs. 21–24) and transverse commissures in stem longitudinal section (Figs. 25–28). Figures 25–27 are from thick sections stained in safranin/alcian green. **21.** Leaf trace in base of sheath, just above its insertion into the stem, metaxylem (mxy) is present but elements are narrow and also continuous with protoxylem (pxy). **22.** Leaf trace in stem periphery close to node of insertion (cf. Fig. 10). Metaxylem is absent, phloem strands are narrow, protoxylem (pxy) represented by numerous, often wide, tracheids and innermost elements ruptured. **23.** Leaf trace close below node of insertion, metaxylem vessels (mxy) well developed and showing associated transition tracheids (arrow heads) of

In juvenile stages a clump of erect shoots is produced (Fig. C), but as the adult canes begin to reach into the tree canopy, a tangled mass of high-climbing shoots is produced (Fig. D). Erect shoots are of uniform diameter (~1.2 cm), except for a slight basal taper in each internode. Internode length is uniform, the measurements for the stem shown in Fig. 42 ($x = 23$ cm, $N = 7$, range 21–26 cm). The juvenile stage lacks climbing organs, but beyond the lowest of five to six above-ground internodes each cane is supported by a series of long whip-like axes with recurved spines that function like grapnels. These are reduced, i.e., unbranched and flowerless inflorescence axes referred to as flagella (Fisher and Dransfield, 1977). Each flagellum originates in the axil of a leaf but is adnate to the stem internode immediately above and to the tubular sheath of the leaf inserted at the next node above, only becoming free just below the mouth of the sheath, where the rachis of the blade diverges. The adnate portion of the flagellum on the stem internode is visible in sections as a cluster of small vascular bundles that become more prominent distally (Fig. 4) and superficially as a longitudinal ridge along the stem. Its position marks the median plane of the subtending leaf and, together with the added notch, is useful in analysis as a point of reference on the stem circumference (Fig. 1). The slight basal taper of each internode, revealed when leaf sheaths are removed, is exaggerated in Figs. 40–43.

Stem anatomy—All major stem histological features of *Calamus* described by Weiner (1992) are present in the species we examined (Figs. 1–6). The epidermis is silicified and the outer wall thickened; stomata are few. The cortex is narrow, often as few as five to ten cells wide at the base of the internode and indistinctly differentiated from the central cylinder (Figs. 2, 4). This outer limit of the central cylinder is represented by a series of subepidermal fibrous strands, sometimes with reduced vascular tissues. They represent the basal continuation of the extensive outer fibrovascular system of the leaf sheath (Fig. 7). Their function is primarily mechanical. The discrete fibrous cortical system found in *Rhapis* (Zimmermann and Tomlinson, 1965) does not exist in the stem internode.

The central cylinder overall is distinguished from that of most palms by the relatively uniform density of its vascular bundles and the wide metaxylem vessels, producing the low density texture of the cane (Figs. 1, 2, 4). There is a narrow outermost region of narrow vascular bundles with somewhat wider fibrous sheaths, but the distinct peripheral bundle density and well-developed fibrous system of most palms is not pronounced. Since fibrous bundle sheaths are of limited development, they contribute minimally to stem texture. The woodiness of the axis results from the ultimate lignification of ground parenchyma cells, whereas the lightness of canes is a result of the well-developed intercellular airspace system (Fig. 3). This produces a “jigsaw puzzle” configuration diagnostic for *Calamus* (Weiner, 1992). Intercellular spaces are bounded by walls that stain prominently in alcian green preparations.

Quantitative features of stem density and changes along individual canes have been provided by Weiner (1992) and Weiner and Liese (1992). The ground tissue includes elongated thin-walled raphide-sacs with short clusters of raphide crystals at wide intervals and somewhat granular mucilaginous cell contents (rs in Figs. 24, 29, 30). The raphide sacs form continuous longitudinal series and since transverse walls are rarely seen in the analyzed videos the impression is given that individual cells are many centimeters long, an impression corrected in longitudinal view. The individual cell lengths (~2 mm) reflect the extended period of internodal elongation (Fisher, 1978) in cell files with infrequent transverse divisions. Tannin cells are scattered and rather infrequent.

Vascular bundles—Vascular bundles are of uniform construction over the greater part of their length in the stem center (Figs. 3, 5, 6), differing only near their level of departure into a leaf as a leaf trace and at their basal discontinuation. This even distribution produces the relatively uniform texture and appearance of the stem in transverse section. Each bundle includes a single prominent metaxylem vessel, >300 μm wide in the largest examples (Figs. 5, 6), with a pair of lateral phloem strands normally with a single series of wide sieve cells, a diagnostic feature for *Calamus*. The phloem strands are enclosed by a narrow band of sheathing fibers continuous only around the phloem side of the bundle. On the inner side of the bundle, i.e., that side directed toward the stem center, is a group of relatively narrow protoxylem elements surrounded by and separated from the metaxylem by conjunctive parenchyma (e.g., Fig. 6). Metaxylem vessels are immediately sheathed by a continuous layer of parenchyma cells with wide pits (Figs. 34, 35). This sheathing parenchyma occupies most of the region adjacent to the wall of the vessel. The histology of the vascular bundle is completed by a peripheral series of discontinuous files of stegmata (silica cells) on the outer side of the bundle sheath fibers.

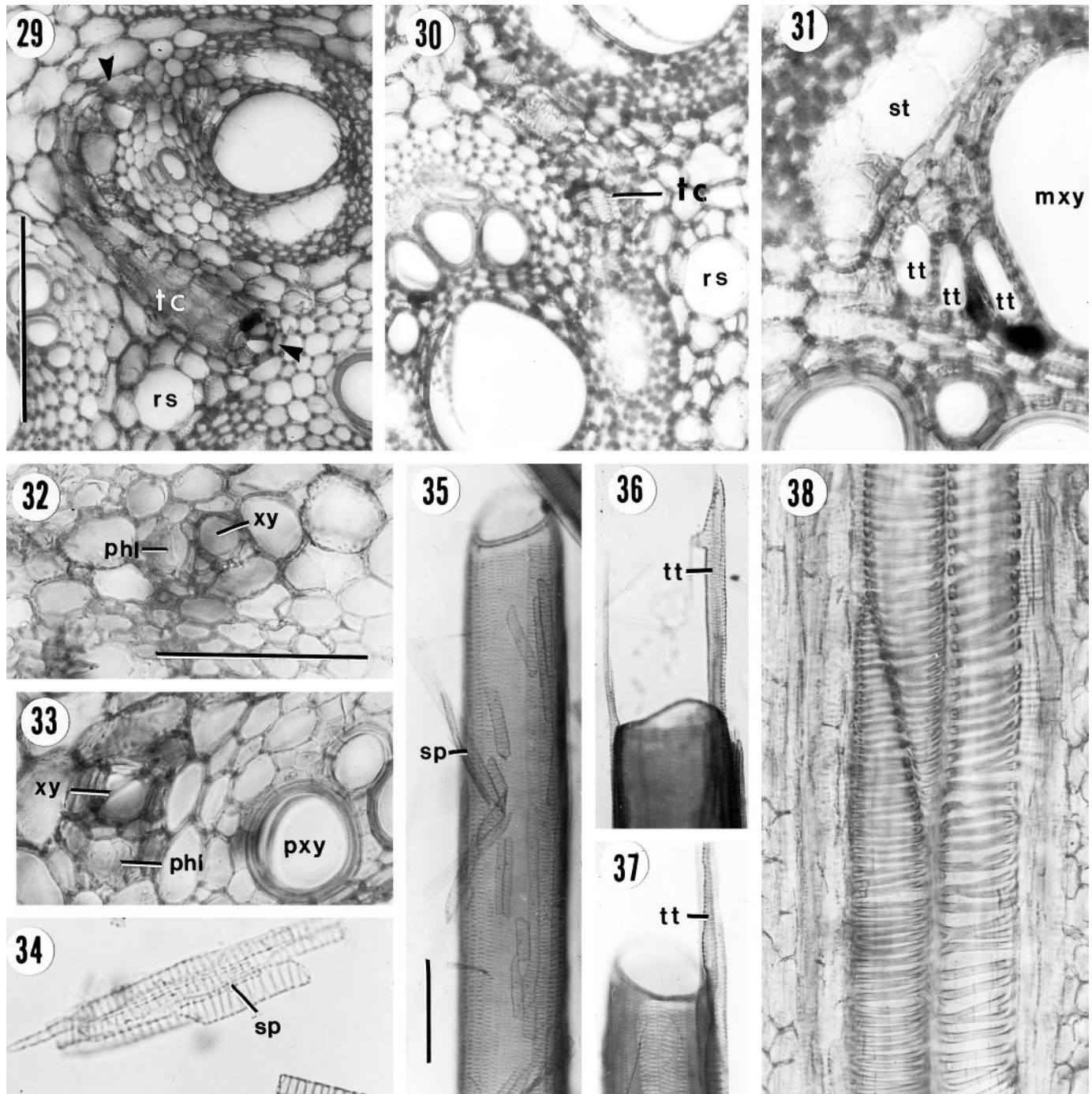
Despite the distinctive appearance of the separated phloem strands in these vascular bundles (Figs. 3, 5, 6), protophloem originates as a single strand opposite the protoxylem, but becomes separated into two strands by sclerification at the original protophloem position as it becomes disrupted by stem elongation.

The change in anatomy along any vascular bundle is described below but attention needs to be drawn to small vascular bundles that are infrequently scattered throughout the ground tissue (arrowheads in Figs. 3 and 5). The narrowest bundles have no protoxylem, a single narrow metaxylem vessel, a narrow phloem strand, and few associated fibers. Surprisingly, the existence of these bundles is not remarked upon by Weiner (1992) even though they are a key component of the vasculature and relate to the major anomalies of this stem.

Tracheary elements—There are three distinct types of tracheary elements in the *Calamus* stem. The wide metaxylem vessels with uniformly and continuously pitted walls are most

←

transverse commissures (cf. Figs. 31, 36, 37). Scale bar = 200 μm . **24.** Stem periphery, with metaxylem of some peripheral bundles (arrows) showing overlapping vessel ends (rs, raphide sac). Scale bar = 200 μm . **25.** Obliquely vertical transverse commissure, phloem (phl) stained more intensely than xylem (xy). **26.** Portion of U-shaped commissure, phloem (phl) stained more intensely than short irregular elements of xylem (xy). **27.** Transverse commissure stained in toluidine blue, phloem (phl) little stained, xylem (xy) of short elements continuous with sheathing parenchyma of axial bundle to left. **28.** Sigmoid transverse commissure with phloem (phl) conspicuously stained. Scale bar = 200 μm . Scale bars for Figs. 21, 22, and 24–27 are the same as for Fig. 23.



Figs. 29–38. *Calamus longipinna*. Transverse commissures in stem transverse section and details of tracheary tissue. **29.** U-shaped commissure (tc) in longitudinal section, but upturned ends (arrow heads) in transverse section (rs, raphide sac). Scale bar = 200 μ m. **30.** Commissure (tc) connecting to lower axial bundle, with well developed sheathing xylem parenchyma (rs, raphide sac). **31.** Commissure at level of insertion on axial bundle, phloem continuous with wide sieve tube (st) and xylem represented by a series of transition tracheids (tt) continuous with wide metaxylem vessel of axial bundle. **32.** Commissure in transverse section with single series of xylem (xy) and phloem (phl) elements; no sheathing fibers. Scale bar = 100 μ m. **33.** Commissure in transverse section with indistinct xylem (xy) and phloem (phl), remote from protoxylem (pxy) of adjacent axial bundle. **34.** Isolated group of sheathing metaxylem vessel parenchyma cells (sp), from maceration, with conspicuously pitted walls. **35.** Isolated vessel element from maceration to show relative dimensions of loosely attached sheathing parenchyma (sp). Scale bar = 200 μ m. **36.** End of vessel element from peripheral bundle to show relative dimensions of transition tracheids (cf. Fig. 31). **37.** Similar vessel elements with attached transition tracheids. **38.** Protoxylem elements from axial bundle with helical wall sculpturing and short, imperforate ends. Scale bar for Fig. 30 is the same as for Fig. 29. Scale bars for Figs. 31, 33 are the same as for Fig. 32. Scale bars for Figs. 36, 37 are the same as for Fig. 35.

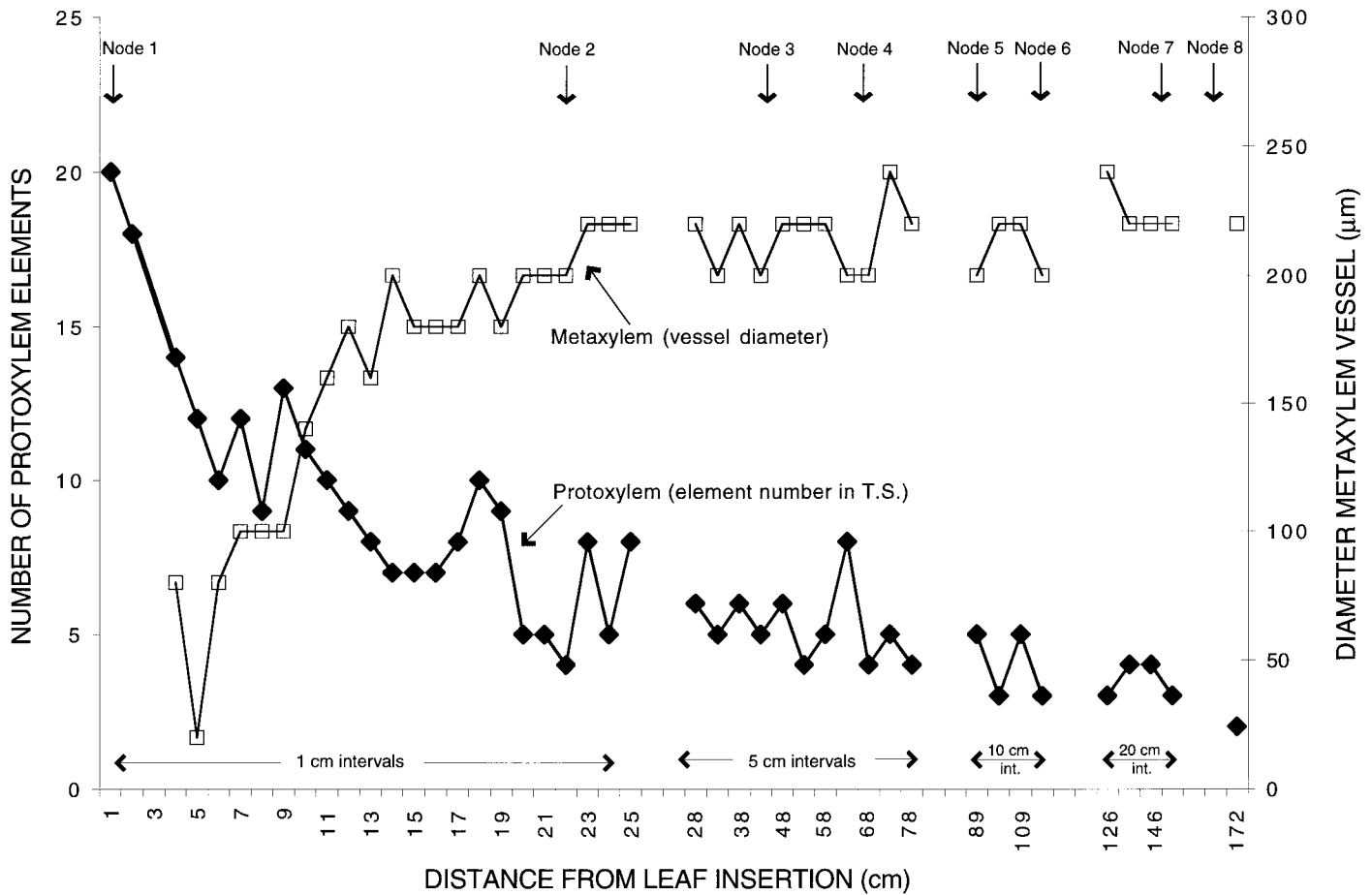


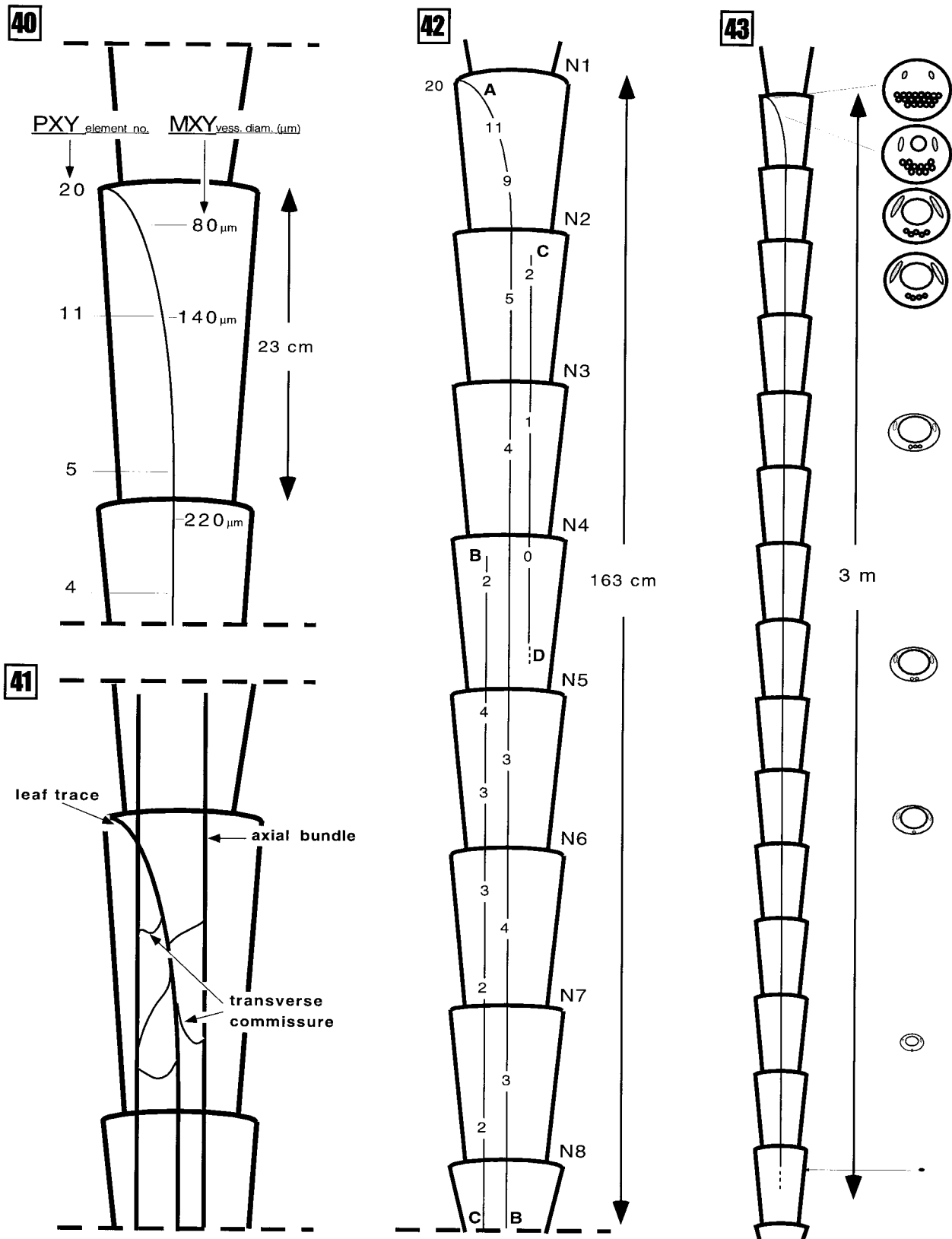
Fig. 39. *Calamus longipinna*. Plot of dimensions of xylem elements from a single axial bundle over a distance of 172 cm and through nearly eight internodes. Distance on x-axis represents distance between successive sections in the series, plotted initially every 1 cm, subsequently (gaps) at increasing intervals of 5, 10, and 20 cm. Metaxylem vessel diameter (in micrometers, scale to right) increases to a maximum and subsequently constant diameter of ~210 µm in the first internode, but the sequence does not include its ultimate decline (cf. Figs. 16–20). Protoxylem element number (as seen in transverse section, scale to left) decreases progressively with increasing distance from the level of insertion, but the sequence does not include its ultimate disappearance (cf. Figs. 17–20).

conspicuous. As mentioned above they are completely sheathed by somewhat elongated parenchyma cells with wide pits. Perforation plates of central vessel elements are always simple with transverse to slightly oblique end walls (Figs. 35–37). The width of the vessels varies considerably in different species. Those illustrated in Fig. 5 have an inside diameter of ~350 µm, but the mean in the material of *Calamus longipinna* that we examined was $210 \pm 13 \mu\text{m}$ ($N = 25$). Vessel element length is in a small range of 1–2 mm. Narrower peripheral bundles have narrow metaxylem vessels, the elements frequently with scalariform perforation plates and with few (up to six) thickening bars on oblique end walls. Protoxylem (Fig. 38) consists of tracheids only, with tapered ends, the wall sculpturing either annular or helical (the helix single or double); annular elements frequently show evidence of extension, with wide separation of successive annuli and their rupture. Protoxylem elements are very variable in length, but up to 3–4 mm long (i.e., longer than the metaxylem vessel elements). Unlike the metaxylem, protoxylem elements are not sheathed continuously with pitted parenchyma cells; at most they make contact with such cells that lie between protoxylem and metaxylem.

The least obvious tracheary elements occur in the transverse commissures and their extensions along the metaxylem vessel

with which they are contiguous. These connecting strands consist of a series of short (50–100 µm) vessel elements with simple perforation plates. They extend into longer, but irregular, elements that are either tracheids or are perforated only at one end, as illustrated by Weiner (1992). She refers to them as transitional elements (Übergangselemente). The difference between transitional elements and sheathing parenchyma is shown best in macerated material, since the former can be seen attached to isolated vessels (Figs. 36, 37), while the latter are clearly much shorter and with simple pits (cf. Fig. 35 and Figs. 36, 37).

Course of vascular bundles—Figures 7–9 represent low magnification transverse views of a sector of the stem surface from the analyzed series. Entering leaf traces are cut somewhat obliquely and are conspicuous by their wide diameter and abundant protoxylem (Fig. 7, arrowheads). About an internode below, the same traces are still easily recognized by the same features (Fig. 8, arrowheads), but now nearer the stem center. In the central region (Fig. 9) there is a complete range of bundle types, i.e., bundles cut at different levels in their axial course. Figures 10–20 recreate histological changes along a single axial strand as they may be described by following a major axial bundle in a basipetal direction. Since any one com-



Figs. 40–43. *Calamus longipinna*. Plots of a single axial bundle and diagram of bundle details. **40.** Detail of xylem dimensions in first internode below insertion of a leaf trace, left-hand values indicate total number of protoxylem elements visible in transverse section, right-hand values indicate diameter of the single wide metaxylem vessel at the three levels indicated. **41.** Interpretative plot (i.e., not to scale) of the frequency of transverse commissures connecting a recently entered leaf trace to adjacent axial bundles in the first internode below its insertion. **42.** Plots of three separate axial bundles at three contrasted levels: A–B represent recently entered leaf trace (numbers indicate total number of protoxylem elements seen in transverse section at different levels), B–C represent a continuing axial bundle, and C–D represent a continuing axial bundle with final loss of protoxylem and its ultimate blind end. **43.** Summary diagram of the

plete central bundle is longer than the section series, the photographs are taken from different bundles at the same level (cf. Fig. 42). To reconstruct a complete bundle additional plots of equivalent bundles were used (as in Figs. 42, 43), i.e., beginning with the same number of protoxylem elements as the discontinued bundle (Fig. 42A–B, B–C, C–D), starting at the top and continuing in the middle of the series. When added top to bottom, the changes that occur in a single bundle can be reconstructed (e.g., Fig. 43).

In the leaf base itself, metaxylem and protoxylem are well developed but not separated (Fig. 21). At the leaf insertion the leaf trace lacks metaxylem and consists of two narrow lateral phloem strands and a complex of numerous protoxylem tracheids of varying diameters (Figs. 10, 22). Sheathing fibers have limited development. This configuration conforms to the general monocotyledon principle that leaves are irrigated solely by protoxylem. As the bundle is followed inward, toward the stem center (i.e., downward) the phloem strands become more conspicuous and xylem in the position of metaxylem (i.e., internal to the protoxylem) becomes evident as an assembly of narrow elements between the phloem strands (Fig. 11). Protoxylem remains well developed, but always well separated from the metaxylem. At progressively lower levels the metaxylem elements become fewer and clustered around a single wider element (Fig. 12). When the bundle reaches the stem center, i.e., its final axial location, the single metaxylem vessel becomes conspicuous and progressively wider (Fig. 13). At the same time the protoxylem elements decrease in number, but not necessarily in diameter. Within a distance of less than two internodes from its level of insertion the bundle adopts the general configuration described for central bundles (Fig. 14). This construction is maintained throughout the major part of the bundle's course and accounts for the overall uniformity of the *Calamus* stem in transverse section. The chief variation is in the number of protoxylem elements, which decreases with increasing distance from the leaf insertion (Figs. 10–16). In peripheral stem regions there is more diversity of stem bundles because of the contrast between recently entered leaf traces and narrow peripheral axial bundles (Fig. 8). The latter represent minor axial bundles which remain near the stem periphery. These have not been plotted.

Continuing in a basal direction, any axial bundle in the stem center decreases in diameter and progressively loses its protoxylem (Figs. 16–20). The bundle finally ends blindly in the ground parenchyma as a strand of elongated but narrow cells, which are either undifferentiated or represented by the remaining fibers of the bundle sheath (Fig. 20). This blind basal ending of axial bundles is the most distinctive feature of the *Calamus* stem (Fig. 43).

Quantitative features—Figure 39 represents the decrease in number of protoxylem elements and increase in metaxylem vessel diameter within a single axial bundle. Since protoxylem is most extensively developed in the distal portion of an axial bundle (Fig. 10) and declines basally (Figs. 11–16), the number of protoxylem elements at any level is a measure of the distance from insertion of any axial bundle. In our most extended section series that includes 8 nodes over a distance of

172 cm with an average internode length of 23 cm ($N = 7$); none of the central axial bundles began and ended within this distance. Figures 39 and 42 therefore represent the change in protoxylem element number in three bundles, where the top of one segment of a lower bundle was matched to the configuration of the lower part of an upper bundle (i.e., A–B, B–C, C–D). By adding head to tail in this way we can arrive at a total distance for a central bundle of ~ 3.0 m (Fig. 43). Since we did not necessarily measure the longest bundle in the axis, this value probably represents an average, rather than a maximum value, as is discussed later. From the average internode length we can see that the sample bundle would have traversed ~ 15 internodes (Fig. 43).

We also observed little regular circumferential displacement of axial bundles so that the axial bundles in the plotted figures are represented in the stem center as straight lines. The internal helix of the *Rhapis* system (Zimmermann and Tomlinson, 1965) was not seen by the methods we used, although it may exist over long distances. Minor bundles, which are the narrower or exclusively fibrous bundles of the leaf sheath, constitute the peripheral system of the axis (Figs. 7, 8). If these bundles have vascular tissue the elements are narrow. The overall length of bundles is also shorter but the repeating pattern of blind-ending bundles is consistent with that of central bundles. This emphasizes the developmental continuum of vascular bundles, from minor to intermediate bundles, as in the *Rhapis* stem.

Transverse commissures—The simple structural plan of Fig. 43 is distinctive because there is no obvious vascular connection among axial bundles and they end blindly in a basipetal direction. The only interconnections among axial bundles are narrow irregular vascular strands, usually with a single sieve tube and vessel, the xylem surrounded by sheathing parenchyma with the same wide pitting that occurs in the sheathing cells of axial metaxylem. Sheathing fibers are totally absent. Transverse commissures are most obvious in thick longitudinal sections (Figs. 25–28) and most easily recognized in permanent, stained preparations. In transverse sections they are easily overlooked (Fig. 32) because they are much narrower than other vascular bundles, with transverse dimensions comparable to the wider protoxylem elements (Fig. 33). The commissures have irregular courses and lengths (cf. Figs. 25 and 27) varying from obliquely longitudinal (Fig. 25) to U- or J-shaped (Fig. 26), to sigmoid (Fig. 28). The tracheary elements are short vessel elements (Fig. 27) with simple perforation plates.

In transverse view it is evident that the course of bundles is not very direct (e.g., Fig. 29) so that complete connections never appear in one section. Figures 30 and 31 show two stages in the fusion of transverse commissures with axial bundles; it is clear that sheathing parenchyma of commissure and axial metaxylem are continuous and that no contact is made with protoxylem. Each connection is marked by the so-called transition tracheids (tt in Fig. 31), which are applied to the wall of the vessel (tt in Figs. 36 and 37).

The transverse commissures are irregularly spaced at intervals of 2–3 mm in an axial direction and are always restricted

←

total plotted distance A–D in Fig. 43. The inset cartoon figures represent the construction of the vascular bundle at progressively lower levels (cf. Figs. 10–20). This diagram summarizes the unique features of *Calamus* vascular anatomy.

to peripheral regions, with most frequent connections between entering leaf traces and peripheral axial bundles. Their presence is most clearly indicated in entering leaf traces by the adnate transition tracheids as narrow tracheary elements contiguous with the metaxylem vessel, as in Figs. 12, 23, and specifically Fig. 31 (tt).

Vessel length—Vessels observed in transverse section are obviously wide, but they are also exceptionally long as is indicated by the absence of obvious vessel ends. In the woody stems of flowering plants, vessel–vessel overlap of tapering ends of two contiguous vessels is seen as a pair of narrow elements in transverse view (Zimmermann, 1971). The absence of this configuration in central bundles is evident in any low-magnification view of a section of a rattan stem (e.g., Figs. 2–5). Paired or grouped vessels in the metaxylem can occur either distally, in which any bundle xylem progressively increases in diameter (Fig. 5), or basally, in which it progressively diminishes. In the distal portion it is not always possible to distinguish the “transition” type of tracheary element, i.e., the xylem extension of a transverse commissure (e.g., Fig. 31) from a short axial vessel. From the absence of vessel ends one can conclude that a single wide metaxylem vessel virtually runs through the whole bundle, as is confirmed in the analytical videos. Since we have established that axial bundles can be ~3 m long, this means that metaxylem vessels are also long. However, they cannot be longer than the total length of any axial bundle. The longest vessels would thus be in the longest major axial bundles. We emphasize that these are maximum values; shorter vessels are certainly present in peripheral axial bundles as can be seen in Fig. 24 (arrows). The main point is that our analysis has revealed a simple structural limit to vessel length.

DISCUSSION

Unique features—Our three-dimensional analysis of the rattan stem shows features that distinguish it from nonclimbing palms. First, axial bundles run independently and without interruption over long distances (measurable in meters) and without any obvious tendency to exhibit a helical pathway. Second, axial bundles are not continuous basally with other axial bundles, but taper gradually and end blindly as a narrow strand of nonvascular cells. Third, there is no direct continuity between protoxylem and metaxylem within a single axial bundle at any level. This contrasts with the situation in the *Rhapis* model in which although metaxylem and protoxylem are discontinuous distally, there is basal continuity (the “vascular insertion” of Zimmermann and Sperry, 1983). Fourth, for most of the length of an axial bundle, the metaxylem is represented by a single wide metaxylem vessel. Since the perforation plates are simple as well as more or less transverse, the major axial pathway for water is a long open tube, its length limited by the length of the axial bundle. Fifth, bridges connecting axial strands in a precise manner, as occur in other palms, are absent. The only connections are by means of transverse commissures that link metaxylem to metaxylem and metaphloem to metaphloem in nearby bundles, restricted to peripheral regions of the stem. The metaxylem connection is made via elongated transitional elements that are narrow and attached directly for some distance to a metaxylem element. These elements have simple perforation plates. With respect to this last feature, Weiner (1992) compared these commissures to

TABLE 1. Structural differences between bridges and transverse commissures.

Features	Bridges (as in <i>Rhapis</i>)	Transverse commissures (as in <i>Calamus</i>)
Course	regular, diverge upward from leaf trace	irregular, diverge upward and downward
Diameter	fairly wide	narrow
Sheathing fibers	present	absent
Axial connection	via overlapping vessels	via transition tracheids
Development	early	late

“bridges” of the *Rhapis* model. However, although they may have the same function as bridges in connecting axial bundles, they are probably not homologous. Structurally, and therefore developmentally, they are different (Table 1). They are best compared with similar commissures that connect axial bundles in palm petioles, although these have been little reported on in the literature and not studied developmentally.

Hydraulic conductivity—The absence of direct continuity from metaxylem to metaxylem of different axial bundles is surprising in view of the requirements for efficient water transport in such long stems, especially as wide vessels imply rapid transport (Ewers, Fisher, and Chiu, 1990). Rattans do have wide vessels, as expected (Klotz, 1978), and the width of metaxylem vessels is positively correlated with stem diameter (Mathew and Bhat, 1997). If there is a relation between vessel diameter and conductivity, rapid transport in rattans can only occur within the metaxylem. Protoxylem transport is less efficient, because elements are narrow, imperforate, and their number progressively decreases basipetally within a single axial bundle.

In the rattan, the normal xylem pathway for water conduction is so modified that there are three considerable resistances to be overcome. First, water can only move from metaxylem to metaxylem via the transverse commissures, which are few and have narrow tracheary elements, even though some have simple perforations. Second, axial water can only move from metaxylem to protoxylem (and hence ultimately into a leaf) across the conjunctive parenchyma sheathing the metaxylem. This is perhaps partly facilitated by the wide pits of the immediate sheathing elements (Fig. 34). Third, the axial metaxylem is tapered at both ends; in particular, the blind ending of the metaxylem in the departing leaf trace, although found in all palms, is very striking because it occurs in a portion of the leaf trace with the maximum amount of protoxylem, in terms of both number and width of elements and yet there is no metaxylem/protoxylem connection. The general observation is that in the rattan stem there are considerable resistances to axial water movement, and movement of water from stem to leaf is also across a considerable resistance.

A possible explanation for the apparent lack of hydraulic efficiency in rattan stems lies in the concept of “safety” vs. “efficiency” within the xylem transport system of plants, i.e., a trade-off between two mutually exclusive tendencies, as described by Zimmermann (1983). Although the construction of the rattan stem, like that of other woody climbers, seems designed for efficient water transport because of the wide vessels, this might be at the risk of permanent loss of transport capacity through frequent vessel cavitation. Since in palms the vasculature cannot be augmented by secondary growth, progressive loss of vessels that become permanently air-filled is clearly

detrimental. Thus the rattan stem is particularly vulnerable to xylem dysfunction, and a high degree of safety may have been built into the system. The structural evidence presented here allows two hypotheses to be developed. First, lack of direct contact between protoxylem and metaxylem may prevent an embolism in leaf protoxylem spreading into stem metaxylem. Leaves are dispensable organs, but the stem is not. Second, if there is a mechanism to refill embolized vessels, it may be facilitated over long distances if there is an appreciable resistance to water flow from vessel to tracheids. The continuous association of vessels and sheathing parenchyma that has wide pits may also facilitate the process. These suggestions must be tested experimentally and indicate the scope for future research. In addition there is considerable evidence that the arborescent palm stem is an efficient water-storage organ as demonstrated by Holbrook and Sinclair (1992a, b). The implication might be that most of the water is stored in parenchyma, but this is not likely in the *Calamus* cane because the vascular bundles are compact and separated by limited ground tissue with well-developed intercellular spaces (Weiner, 1992). Instead, the metaxylem may be primarily a water-storage tissue. It is notable that the amount of stem occupied by vessels may be as much as 30% total stem volume (e.g., Fig. 2). Such speculative ideas are not helpful in the present state of our knowledge, but at least we have drawn attention to a type of stem with remarkable and counterintuitive features, even though the organ is clearly very successful. Similar considerations may be extended to a number of other climbing monocotyledons, as suggested by Tomlinson and Fisher (2000).

LITERATURE CITED

- BAKER, W. J., J. DRANSFIELD, M. M. HARLEY, AND A. BRUNEAU. 1999. Morphology and cladistic analysis of subfamily Calamoideae (Palmae). In A. Henderson and F. Borschenius [eds.], *Evolution, variation, and classification of palms. Memoirs of the New York Botanical Garden* 83: 1–324.
- BHAT, K. M., W. LIESE, AND U. SCHMITT. 1990. Structural variability of vascular bundles and cell walls in rattan stems. *Wood Science and Technology* 24: 221–224.
- BURKILL, I. H. 1966. A dictionary of the economic products of the Malay Peninsula, 2 vols. 2nd ed. Ministry of Agriculture and Cooperative, Kuala Lumpur, Malaysia.
- EWERS, F. W., J. B. FISHER, AND S. T. CHIU. 1990. A survey of vessel dimensions in stems of tropical lianas and other growth forms. *Oecologia* 84: 544–552.
- FISHER, J. B. 1978. A quantitative description of shoot development in three rattan palms. *Malaysian Forester* 41: 280–293.
- , AND J. DRANSFIELD. 1977. Comparative morphology and development of inflorescence adnation in rattan palms. *Botanical Journal of the Linnean Society* 75: 119–140.
- HOLBROOK, N. M., AND T. R. SINCLAIR. 1992a. Water balance in the arborescent palm, *Sabal palmetto*. I. Stem structure, tissue water release properties and leaf epidermal conductance. *Plant, Cell and Environment* 15: 393–399.
- , AND ———. 1992b. Water balance in the arborescent palm *Sabal palmetto*. II. Transpiration and stem water storage. *Plant, Cell and Environment* 15: 401–409.
- KLOTZ, L. H. 1978. Observations on diameter of vessels in stems of palms. *Principes* 22: 99–106.
- MATHEW, A., AND K. M. BHAT. 1997. Anatomical diversity of Indian rattan palms (Calamoideae) in relation to biogeography and systematics. *Botanical Journal of the Linnean Society* 125: 71–86.
- TOMLINSON, P. B. 1990. The structural biology of palms. Oxford University Press, Oxford, UK.
- . 1995. Non-homology of vascular organisation in monocotyledons and dicotyledons. In P. J. Rudall, P. J. Cribb, D. F. Cutler, and C. J. Humphries [eds.], *Monocotyledons: systematics and evolution*, 589–682. Royal Botanic Gardens, Kew, UK.
- , AND J. B. FISHER. 2000. Stem vasculature in climbing monocotyledons: a comparative approach. In K. L. Wilson and D. A. Morrison [eds.], *Monocotyledons—systematics and evolution*, vol. 1. Proceedings of the Second International Conference on the Comparative Biology of the Monocotyledons, September 1998. CSIRO, Melbourne, Australia.
- , AND M. H. ZIMMERMANN. 1966. Anatomy of the palm *Rhapis excelsa*. II. Rhizome. *Journal of the Arnold Arboretum* 47: 248–261.
- UHL, N. W., AND J. DRANSFIELD. 1987. *Genera palmarum*. Allen Press, Lawrence, Kansas, USA.
- WEINER, G. 1992. Zur Stammanatomie der Rattanpalmen. Ph.D. dissertation, University of Hamburg, Hamburg, Germany.
- , AND W. LIESE. 1992. Zellarten und Faserlängen innerhalb des Stammes verschiedenen Rattangattungen. *Holz als Roh- und Werkstoff* 50: 457–464.
- , AND ———. 1993. Generic identification key to rattan palms based on stem anatomical characters. *Journal of the International Association of Wood Anatomists* 14: 55–61.
- ZIMMERMANN, M. H. 1971. Dicotyledonous wood structure (made apparent by sequential sections). In G. Wolf [ed.], *Encyclopaedia cinematographica*. Institut für den Wissenschaftlichen Film, Göttingen, Germany.
- . 1983. Xylem structure and the ascent of sap. Springer Verlag, Heidelberg, Germany.
- , K. F. MCCUE, AND J. S. SPERRY. 1982. Anatomy of the palm *Rhapis excelsa*. VIII. Vessel network and vessel-length distribution in the stem. *Journal of the Arnold Arboretum* 63: 83–95.
- , AND J. S. SPERRY. 1983. Anatomy of the palm *Rhapis excelsa*, IX. Xylem structure of the leaf insertion. *Journal of the Arnold Arboretum* 64: 599–609.
- , AND P. B. TOMLINSON. 1965. Anatomy of the palm *Rhapis excelsa*. I. Mature vegetative axis. *Journal of the Arnold Arboretum* 46: 160–180.
- , AND P. B. TOMLINSON. 1966. Analysis of complex vascular systems in plants: optical shuttle method. *Science* 152: 72–73.